

Application of graph theory to cost-effective fire protection of chemical plants during domino effects

Khakzad Rostami, Nima; Landucci, G; Reniers, Genserik

DOI

[10.1111/risa.12712](https://doi.org/10.1111/risa.12712)

Publication date

2016

Document Version

Accepted author manuscript

Published in

Risk Analysis: an international journal

Citation (APA)

Khakzad Rostami, N., Landucci, G., & Reniers, G. (2016). Application of graph theory to cost-effective fire protection of chemical plants during domino effects. *Risk Analysis: an international journal*. <https://doi.org/10.1111/risa.12712>

Important note

To cite this publication, please use the final published version (if applicable). Please check the document version above.

Copyright

Other than for strictly personal use, it is not permitted to download, forward or distribute the text or part of it, without the consent of the author(s) and/or copyright holder(s), unless the work is under an open content license such as Creative Commons.

Takedown policy

Please contact us and provide details if you believe this document breaches copyrights. We will remove access to the work immediately and investigate your claim.



**Application of graph theory to cost-effective fire protection
of chemical plants during domino effects**

Journal:	<i>Risk Analysis</i>
Manuscript ID	RA-00117-2016
Wiley - Manuscript type:	Original Research Article
Key Words:	Domino effect, Fire protection, Graph theory

SCHOLARONE™
Manuscripts

Peer Review

1
2
3
4
5
6
7
8
9
10
11
12
13
14
15
16
17
18
19
20
21
22
23
24
25
26
27
28
29
30
31
32
33
34
35
36
37
38
39
40
41
42
43
44
45
46
47
48
49
50
51
52
53
54
55
56
57
58
59
60

**Application of Graph Theory to Cost-effective Fire Protection of
Chemical Plants During Domino Effects**

For Peer Review

Abstract

In the present study, we have introduced a methodology based on graph theory and multi-criteria decision analysis for cost-effective fire protection of chemical plants subject to fire-induced domino effects. By modeling domino effects in chemical plants as a directed graph, the graph centrality measures such as out-closeness and betweenness scores can be used to identify the installations playing a key role in initiating and propagating potential domino effects. It is demonstrated that active fire protection of installations with the highest out-closeness score and passive fire protection of installations with the highest betweenness score are the most effective strategy in reducing the vulnerability of chemical plants to fire-induced domino effects. We have employed a dynamic graph analysis to investigate the impact of both the availability and the degradation of fire protection measures over time on the vulnerability of chemical plants. The results obtained from the graph analysis can further be prioritized using multi-criteria decision analysis techniques such as the method of reference point to find the most cost-effective fire protection strategy.

Keywords

Domino effect; Fire protection; Quantitative risk assessment; Graph theory; Multi-criteria decision making.

1. INTRODUCTION

Domino effects have been responsible of several catastrophic accidents which took place in the chemical and process industry.⁽¹⁻⁶⁾ The high destructive potential of domino effects is widely recognized,⁽⁷⁻¹¹⁾ hence technical standards and legislation concerned with the control of major accident hazards include measures to assess, control and prevent domino effects.⁽¹²⁾

Pioneering approaches for the assessment of domino effects, mostly developed in the 1980s and 1990s,^(2,7,13-16) were based on oversimplifying assumptions, without accounting for either the actual process of equipment damage or the possible mitigation due to in-place safety barriers. More recent studies were aimed at developing probabilistic models to evaluate the failure probability of equipment involved in domino events,⁽¹⁷⁻²³⁾ leading to notable improvement in the risk assessment of domino effects.⁽²⁴⁻²⁶⁾ In other research lines, more advanced mathematical tools such as Monte Carlo simulations⁽²⁷⁾ or Bayesian networks⁽²⁸⁻³⁰⁾ were adopted. However, in none of these methodologies the effect of safety barriers was taken into account. Nevertheless, in order to support a more comprehensive assessment of domino effects, the quantitative analysis of the safety barriers is a critical issue.

As remarked by Janssens et al.⁽³¹⁾ research studies dealing with the safety analysis of domino effects have mainly focused on an inherent safety management of domino effects, especially through dedicated index methodologies.⁽³²⁻³⁵⁾ Inherent safety measures are effective at the design stage⁽³⁶⁻³⁹⁾ and may constitute an optimal strategy to limit the occurrence of domino effects, for example, through appropriate ranking of equipment and layout definition.^(32,40,41) Nevertheless, for existing industrial facilities, equipment replacement or layout modification is not easily achievable, due to relevant cost and space constraints, especially in industrial clusters.⁽⁴²⁻⁴⁴⁾

Aside from inherently safer design, engineering active and passive safety barriers – also known as add-on safety barriers – are of utmost importance in the prevention, control, and mitigation of domino effects. Landucci et al.^(45,46) introduced the dual nature of add-on safety barriers, addressing the availability and effectiveness thereof, providing a repository of data for different

1
2
3 types of active, passive and procedural barriers.^(47,48) Nevertheless, the allocation of add-on
4 safety measures and the optimization of their configuration considering their performance have
5 never been dealt with. This constitutes a relevant research task to improve vulnerability,
6 robustness, and resilience profile of industrial facilities against domino effect propagation,<sup>(35,49-
7 51)</sup> which still needs to be explored.

8
9
10
11
12 According to the definition provided in,⁽⁴⁹⁾ vulnerability can be defined as the capability of
13 fostering either the onset or the escalation of potential domino effects, both considering
14 individual equipment or an entire plant. In recent attempts, Khakzad and Reniers^(49,52)
15 demonstrated the application of graph theory to vulnerability assessment of tank farms subject
16 to domino effects. They identified the efficacy of a set of graph metrics in both unit and plant-
17 wide vulnerability analysis of process plants. The graph metrics were identified as an effective
18 screening tool aimed at identifying the most critical units and the plant layout configurations
19 with respect to the escalation of domino effects. Nevertheless, the effect of protection systems
20 was not considered in the methodology.

21
22
23
24
25
26
27
28
29
30
31
32 The present work is aimed at evaluating the vulnerability of process plants subject to fire-
33 induced domino effects, i.e., domino effects not only triggered by fire but also involving fires
34 (“fired” domino effect⁽⁵³⁾) are taken into consideration and modeled through a graph theory
35 application. The effect of relevant types of active and passive fire protection systems is
36 implemented in the model in order to obtain a more realistic vulnerability profile. The dynamic
37 degradation of the involved fire protection systems and its impact on the domino effects are also
38 considered in the analysis. In order to demonstrate the efficacy and practicality of the
39 methodology, it is applied to a real case study. The results obtained from the graph theory
40 modeling are further analyzed using a multi-criteria decision making technique to determine
41 the most cost-effective fire protection strategy.

52 53 54 **2. METHODOLOGY**

55 56 **2.1 Overview**

Fig. 1 shows the methodology adopted in this work for the vulnerability assessment of industrial facilities to domino effects accounting for safety barriers.

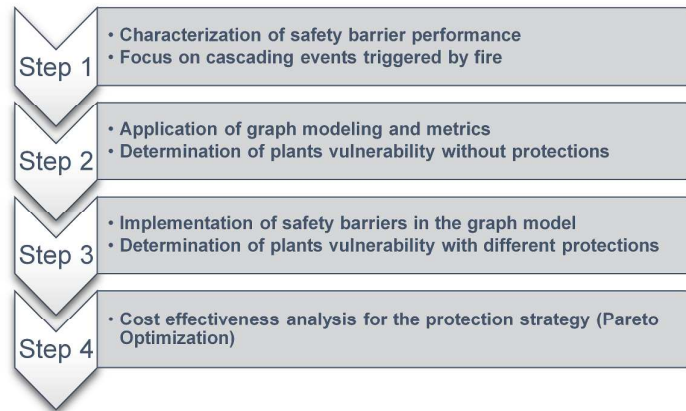


Figure 1: Overview of the methodology adopted in the present work.

The initial step of the methodology (step 1 in Fig. 1) is devoted to the characterization of the relevant safety barriers commonly used for the prevention or mitigation of escalation in the chemical and process industry. The focus of this work is the study of domino effects triggered by fire, but the framework may be extended to other types of domino escalation (e.g., caused by overpressure or fragments). In Section 2.2 the relevant safety barriers considered in the present study are collected; their protective action is characterized; and they are implemented in the graph theory model (step 2 in Fig. 1). The graph model, presented in Section 2.3, enables one to determine the graph metrics such as closeness and betweenness centrality scores for the quantification of plant vulnerability to domino effects in the presence of safety barriers (step 3 in Fig. 1). Different protection configurations and dynamic evolution of potential domino effects are modeled through graph theory. Since graph theory is based on deterministic assumptions,⁽⁵⁴⁾ uncertainties and failure probabilities are not considered in the present work. Finally, in Step 4 of the methodology (see Fig. 1) a cost-effectiveness analysis is carried out in order to compare the benefit gained in the form of plant vulnerability reduction versus the cost of respective protection configurations (i.e., added safety measures). For this purpose, the method of reference point – a Pareto optimization – is employed in Section 2.4.

2.2 Safety barriers quantitative assessment

Generally speaking, fire protection safety barriers are aimed at delaying or preventing accident escalation during fire-induced domino effects. The procedure for their quantitative implementation in the graph theory model is thus different, depending on their desired protective action. Therefore, a preliminary characterization of such safety barriers needs to be carried out.

According to the classification proposed by CCPS⁽⁴⁷⁾ and the ARAMIS project,⁽⁴⁸⁾ three different categories of safety barriers against fire-induced domino events may be identified: i) active protection systems; ii) passive protection systems; iii) procedural and emergency measures. In the present work, we addressed only the first two barrier types, excluding the procedural and emergency response measures. This is due to the relevant uncertainties associated to human factors in the performance of emergency response teams,⁽⁵⁵⁻⁵⁷⁾ requiring a probabilistic approach which is out of the scope of the present study.

2.2.1 Passive protection systems

A generic passive protection device is a system or a barrier which does not require either power or external activation to trigger the protection action.^(3,48,58) In the framework of escalation prevention, the application of fireproofing materials is a relevant and effective safety barrier,^(40,41,59,60) due to the shielding effect which reduces the incoming fire heat flux, and consequently the vessel heat-up. This allows to delay the time to reach the critical conditions leading to the failure of the exposed target.^(61,62) There are several types of passive fire protection materials which can be selected in order to provide storage and process equipment with effective protection:⁽⁵⁹⁾

- Cementitious products generally based on Portland cement plus lightweight aggregates (vermiculite sprays);
- Intumescent coatings generally epoxy based, spray or hand applied;

1
2
3 - Blanket systems made from man-made fibers which use insulation as their primary fire
4 protection mechanism.
5

6
7 The above-mentioned materials can be considered as high performance protection, since they
8 are specifically designed to withstand severe fire conditions, being able to protect process
9 equipment for about 120 min in an engulfing hydrocarbon pool fire.^(40,45)
10

11
12 Therefore, in order to implement fireproofing protection (passive fire protection) in the graph
13 model, it is assumed that a fireproofed tank cannot be entailed in the domino effects for a given
14 rating time, (e.g., the fireproofed tank receives no heat flux). This assumption was made by
15 Khakzad and Reniers in a previous work,⁽⁴⁹⁾ but without considering the possible inefficiency of
16 the heat resistant coating and possible degradation phenomena. As a matter of fact, fireproofing
17 coatings exhibit a dynamic degradation during fire exposure. In some cases, such as for
18 intumescent coatings or cementitious materials, phenomena of devolatilization, expansion,
19 swelling, etc., are inherent part of the protective action. Nevertheless, for prolonged fire
20 exposure, the degradation and loss of efficiency of fireproofing coatings have been documented
21 in experimental and modeling studies.^(60,63-65) In order to account for these complicating
22 phenomena in the graph model, it is assumed that only a limited fraction of the nominal rating
23 time (120 min) is guaranteed with optimal performance, according to work of Landucci et
24 al.^(45,46)
25

26
27 - for exposure time lower than or equal to 60 min, the fireproofed tank receives no heat flux
28 (complete shielding effect);
29

30
31 - for exposure time higher than 60 min, it is conservatively assumed that the fireproofed tank
32 receives the full heat load due to the fire as in the absence of fireproofing.
33

34
35 If other material types are used for equipment protection, such as common insulants (glass
36 wool, rock wool, etc.) not designed for fireproofing applications, it is assumed that no shielding
37 effect can be achieved, implying that the target tank receives the full heat load due to the fire.
38
39
40
41
42
43
44
45
46
47
48
49
50
51
52
53
54
55
56
57
58
59
60

2.2.2 Active protection systems

Active protection systems are barriers which require external activation to perform their protective effect.^(47,48) Typically, an active protection system is composed of three sub-systems in series: i) a fire/smoke detection system; ii) a treatment system (logic solver, releasing panel or alarm advising operator); iii) an actuation system (mechanical, instrumented, human etc.), aimed at performing the protective action.

The protective action may be devoted to the prevention or suppression of the primary fire, either by limiting the amount of released flammable substance as in the case of emergency shut-down or venting the potential target equipment as in the case of emergency blow-down. Usually, such systems are part of the general loss prevention measures of the plant.⁽³⁾

The present work is devoted to the characterization of systems for the delivery of fire-fighting agents (such as water or water-based foam), providing effective control of the primary fire and prevention its spread to nearby units (fire-fighting agent delivery systems).

These systems constitute a widely used solution for the protection of atmospheric floating roof tanks storing flammable liquids, according to international standards and current industrial practice.⁽⁶⁶⁻⁷⁰⁾ The performance of such protection systems has been extensively documented by experimental and numerical studies.⁽⁷¹⁻⁷³⁾ Although the aim of this type of protection is to control or, eventually, suppress the primary fire, it usually is conservatively assumed that active fire protection measures mitigate the radiation emitted from the flame, without suppressing the fire. In particular, the mitigated flame emissive power (Q_m) associated with the fire in a tank due to active fire protections can be computed as follows:

$$Q_m = (1 - \eta \times \varphi) \times Q_f \quad (1)$$

in which Q_f is the flame emissive power in the absence of mitigation; φ is the radiation reduction factor, and η is an efficiency parameter. An average value of $\varphi = 60\%$ for a flame assimilated as a black body at 1100K may be achieved due to water mist mitigation.^(74,75) In the present study, a conservative efficiency value of $\eta = 75\%$ is considered to quantify Eq. (1).

1
2
3 It is worth to mention that the firefighting agents may be provided only for a given time, based
4 on the total amount of water/foam and the required flowrate to control or suppress the fire.
5 According to common industrial practice and standards for the petroleum industry, water is
6 provided for 4 to 6 hours at the maximum flowrate.^(69,76) However, in a survey carried out in
7 Oil&Gas production facilities, 2 hours is usually taken into account. Hence, in order to provide
8 conservative indications, a maximum duration of 2 hours (120 min) is assumed as the operative
9 time in which active measures, once activated, provide the necessary amount of water to control
10 the primary fire. In other words, Eq. (1) is valid only for 120 min; after 120 min, the fire is no
11 longer mitigated, the flame emits the unmitigated heat flux Q_f towards the targets till the flame
12 (tank) burns out.
13
14
15
16
17
18
19
20
21
22
23

2.3 Graph theory application

2.3.1. Definitions

24
25
26
27
28
29 A mathematical graph is a set of vertices (nodes) and edges, in which an edge connects two
30 nodes. Depending on whether the edges are directed or undirected, the graph is directed or
31 undirected, respectively. Likewise, a graph can be weighted or unweighted; in a weighted graph,
32 a variety of numerical attributes can be assigned to either the nodes or edges of the graph. Thus,
33 a weighted graph can be presented as $G = (V, E, W_V, W_E)$ where V is a set of nodes, E is a set of
34 edges, while W_V and W_E represent the sets of weights attributed with the vertices and edges,
35 respectively.
36
37
38
39
40
41
42
43

44 In a directed graph, a walk from the node v_i to v_j is a sequence of connected nodes starting from
45 v_i and ending in v_j when each intermediate node can be traversed several times. A path,
46 however, is a walk in which each intermediate node can be traversed at most once. Accordingly,
47 the geodesic distance (hereafter, distance) between v_i and v_j , denoted as d_{ij} is the length of the
48 shortest path from v_i to v_j . In an unweighted graph, the distance is simply the number of edges
49 constituting the shortest path, whereas in a weighted graph it is equal to the sum of the weights
50
51
52
53
54
55
56
57
58
59
60

of the involved edges in the shortest path. Conventionally, if there is no path between v_i and v_j , then $d_{ij} = \infty$.

Based on the concept of distance, a number of graph metrics have been developed to investigate the characteristics of graphs, among which betweenness and closeness centrality scores⁽⁵⁴⁾ are very popular. The betweenness of a node, denoted as $C_b(v_i)$, is defined as the ratio of the distances between all pairs of other nodes (i.e., between v_j and v_k so that $i \neq j \neq k$) which traverse v_i , denoted as $d_{jk}(v_i)$, to the total distance within the graph regardless of whether or not they traverse v_i :

$$C_b(v_i) = \sum_{j,k} \frac{d_{jk}(v_i)}{d_{jk}} \quad (2)$$

Among the nodes of a graph, the nodes with relatively higher betweenness scores lie along a larger fraction of paths within the graph, thus their removal (or isolation) from the graph can cause large disconnection.⁽⁴⁹⁾ The closeness of a node, $C_c(v_i)$, can be defined as the number of steps needed to reach every other node of the graph from v_i – also known as out-closeness $C_{c-out}(v_i)$ – or to access v_i from every other node of the graph – also known as in-closeness $C_{c-in}(v_i)$:

$$C_{c-out}(v_i) = \frac{1}{\sum_j d_{ij}} \quad (3)$$

$$C_{c-in}(v_i) = \frac{1}{\sum_j d_{ji}} \quad (4)$$

Based on the centrality scores of vertices given in Eq.s (2)-(4), the average centrality scores of the entire graph (i.e., graph-level centrality scores) can be measured.

2.3.2. Chemical plant as a graph

Representing the major hazardous installations¹ (MHIs) of a chemical plant as the vertices and the escalation vectors such as heat radiation and explosion overpressure as the edges, the plant can be modeled as a directed graph.⁽⁴⁹⁾ For illustrative purposes, consider a chemical storage plant shown in Fig. 2a, comprising four atmospheric storage tanks the characteristics of which

¹ Major hazardous installations are attributed with large inventory of flammable or explosive chemical substances, e.g., storage tanks. Such units are further categorized as lower-tier and upper-tier installations in Seveso Directive, based on whether their chemical containment is lower or higher than a predefined threshold, respectively.

are listed in Table I. Assuming the pool fire as the most credible accident scenario and also a prevailing atmospheric condition including a weather temperature of 15°C, a relative humidity of 25%, a wind gusting with a speed of 2 m/s from North, and the stability class F, the magnitudes of heat radiation intensities are calculated as shown in columns 2-5 of Table II. It, however, should be noted that for a heat radiation to cause damage to neighboring units its intensity should be higher than a threshold value of $Q_{th} = 10 \text{ kW/m}^2$.⁽²⁴⁾ Credible heat radiation intensities have been displayed with bold numbers in Table II. As a result, the chemical plant of Fig. 2a can be represented as a directed graph in Fig. 2a.

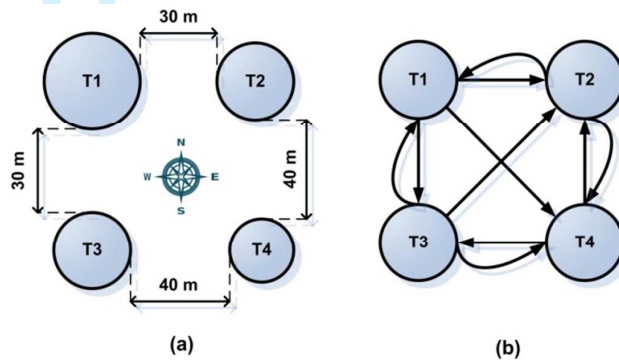


Figure 2. a) Layout of a hypothetical chemical storage plant; b) representation of the plant and the respective heat radiations in Table II as a directed graph.

Table I. Characteristics of the storage tanks in Fig. 2a.

Tank	Substance	Diameter (m)	Height (m)	Volume (m ³)
T1	Benzene	40	10	12000
T2	Acetone	30	10	6000
T3	Toluene	30	10	6000
T4	Toluene	20	10	2500

Table II. Heat radiation (kW/m²) received by tank T(j) due to a pool fire in tank T(i) in Fig. 2b, and the centrality scores.

	T1	T2	T3	T4	C_b	C_{c-out}
T1	NA	36.3	36.3	20.6	0.17	2.86
T2	11.2	NA	5.21	11.2	0	1.02
T3	27.9	15.8	NA	27.9	0.17	2.22
T4	5.50	17.4	17.4	NA	0	1.45
Graph	-	-	-	-	-	1.89

1
2
3 Modeling the chemical plant as a graph, a number of graph metrics can be employed to
4 investigate the vulnerability of both the units and the entire plant in the context of domino
5 effects. In this regard, Khakzad and Reniers⁽⁴⁹⁾ demonstrated that primary events (fires or
6 explosions) in the installations (vertices) with higher C_{c-out} scores are more likely to propagate
7 throughout the plant, resulting in more severe and widespread domino effects. Likewise, the
8 installations with higher C_b scores facilitate the propagation of a primary event or an ongoing
9 domino effect better than those with lower C_b scores. It was also ascertained that among similar
10 chemical plants – similar both in terms of the number of identical MHIs and the amount of
11 contained chemicals – the plant with the highest graph-level out-closeness score is more
12 susceptible to domino effects.⁽⁴⁹⁾

13
14 Modeling the graph of Fig. 2b using igraph package⁽⁷⁷⁾ in R programming software⁽⁷⁸⁾, the
15 quantities of the C_b and C_{c-out} scores of the storage tanks have been calculated as listed in the
16 columns 6 and 7 of Table II. The graph-level C_{c-out} score can thus be calculated as the arithmetic
17 average of the respective node-level C_{c-out} scores. As can be seen from Table II, T1 and T3 are
18 attributed to the highest C_{c-out} and C_b scores.

19
20 In the present study, we modeled the graph of Fig. 2b as a weighted graph in the sense that the
21 intensities of the heat radiation vectors were taken into account as the weight of the
22 corresponding edges. In weighted graphs, a larger weight for an edge basically implies a longer
23 distance between the two nodes connected by the edge, and thus representing a weaker
24 interaction between the nodes. Thus, we assigned the weight of each edge as the ratio of the
25 threshold value, $Q_{th} = 10 \text{ kW/m}^2$, and the actual value of the heat radiation associated with the
26 edge. For example, in the graph of Fig. 2b, the weight of the edge from T1 to T2 is $\frac{10}{36.3} = 0.28$
27 while that of the edge from T2 to T1 is $\frac{10}{11.2} = 0.89$. That is, given a pool fire in either tank, T2 can
28 be reached (impacted) by T1 sooner (more severely) than T1 can be reached by T2, because of
29 the shorter distance of the former (0.28 versus 0.89).

30 31 32 33 34 35 36 37 38 39 40 41 42 43 44 45 46 47 48 49 50 51 52 53 54 55 56 57 58 59 60 *2.3.3. Modeling of safety barriers*

1
2
3 To investigate the impact of the safety barriers discussed in Section 2.2 on the vulnerability of
4 chemical plants to domino effects, a dynamic approach is adapted here by dividing the time line
5 into three intervals, namely [0, 60 min), [60 min, 120 min), and [120 min, ∞). The first time
6 interval is when both passive (fireproof coating) and active (water sprinklers) safety barriers
7 are in effect, neglecting the failure probabilities of either safety barrier (i.e., availability =
8 100%). The second time interval is, however, characterized by the degradation of the passive
9 fire protection (see Section 2.2.1) whereas the active fire protection is still in effect. The last
10 time interval is when neither the passive nor the active fire protection is in operation; the latter
11 is due to the depletion of the water/water-based foam reservoirs (see Section 2.2.2). In other
12 words, the corresponding graph representation of the storage plant in the last time interval will
13 be as Fig. 2b provided that none of the tanks has burned out yet.

14
15
16
17
18
19
20
21
22
23
24
25
26 To investigate the most effective allocation of passive and active safety barriers, a number of
27 cases are considered, assuming that both active and passive fire protections can be employed
28 once:

- 29 • Case 1: T1 is both actively and passively protected;
- 30 • Case 2: T1 is actively protected while T3 is passively protected;
- 31 • Case 3: T1 is passively protected while T3 is actively protected;
- 32 • Case 4: T1 is passively protected while T2 is actively protected.

33
34
35
36
37
38
39
40
41
42
43
44
45
46
47
48
49
50
51
52
53
54
55
56
57
58
59
60
Generally speaking, the fireproof coating of a tank does not preclude the possibility of a pool fire
at the tank. Fig. 3 displays the chronological changes of the graphs associated with the storage
plant of Fig. 2a under the four safety allocation cases mentioned above. The double-outlined
nodes represent fireproofed (passively protected) tanks while dashed edges originating from a
node stand for attenuated heat radiations due to the active protection of the node (tank).

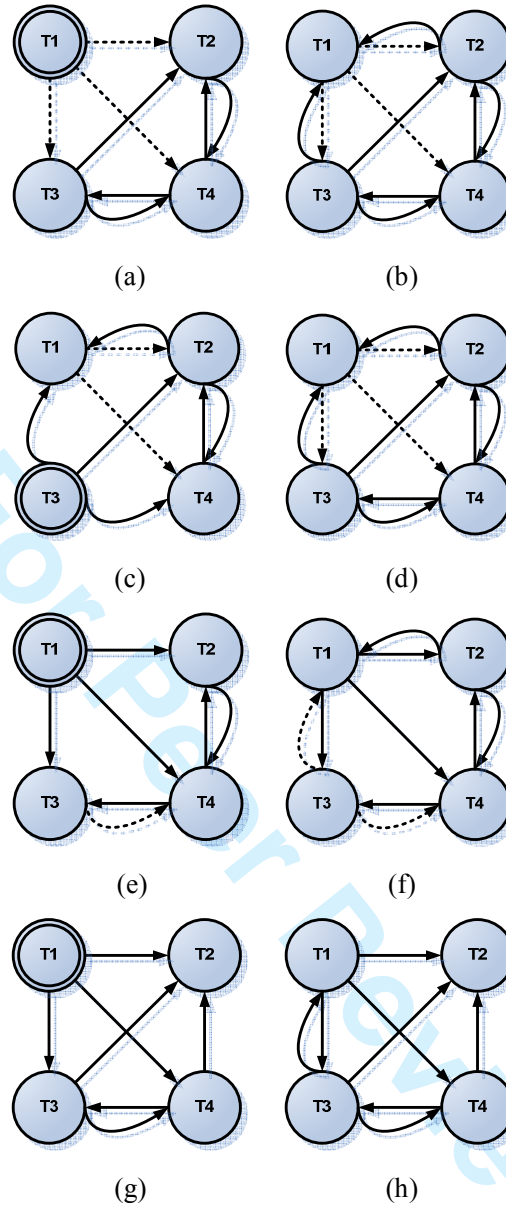


Figure 3: Graph representation of the storage plant in Fig. 2a under safety allocation scenarios the four different considered cases: a) case 1, $t \in [0, 60 \text{ min}]$; b) case 1, $t \in [60 \text{ min}, 120 \text{ min}]$; c) case 2, $t \in [0, 60 \text{ min}]$; d) case 2, $t \in [60 \text{ min}, 120 \text{ min}]$; e) case 3, $t \in [0, 60 \text{ min}]$; f) case 3, $t \in [60 \text{ min}, 120 \text{ min}]$; g) case 4, $t \in [0, 60 \text{ min}]$; h) case 4, $t \in [60 \text{ min}, 120 \text{ min}]$. For the last time interval $[120 \text{ min}, \infty)$, the graph will be as shown in Fig. 2b, if none of the tanks has burned out.

The updated quantities of the heat radiation intensities due to the implementation of the passive and active safety barriers along with the values of C_b and C_{c-out} for the graphs of Fig. 3 have been tabulated in Table III. For the sake of better illustration, the graph-level out-closeness scores for the three consecutive time intervals have been compared in Fig. 4, indicating the

outperformance of Case 1 in reducing the out-closeness of the graph and thus in decreasing the vulnerability of the storage plant to domino effects.⁽⁴⁹⁾ This result not only is in agreement with the work of Khakzad and Reniers⁽⁴⁹⁾ regarding the importance of the fireproofing of installations with the highest C_b (T1 and T3 in this example) but also goes one step further by demonstrating the influence of the active protection of installations with the highest C_{c-out} (T1 in this example) on the vulnerability of the plant.

Table III. The updated heat radiation intensities and the centrality scores for the graphs in Fig. 3.

Case 1	$0 \leq t < 60 \text{ min}$						$60 \leq t < 120 \text{ min}$							
	T1	T2	T3	T4	C_b	C_{c-out}	T1	T2	T3	T4	C_b	C_{c-out}		
T1	NA	19.97	19.97	11.33	0	1.61	NA	19.97	19.97	11.33	0.17	1.61		
T2	0	NA	5.21	11.2	0	0.47	11.2	NA	5.21	11.2	0	0.95		
T3	0	15.8	NA	27.9	0.17	0.6	27.9	15.8	NA	27.9	0.33	2.22		
T4	0	17.4	17.4	NA	0.17	0.58	5.5	17.4	17.4	NA	0	1.45		
Graph													0.82	1.56
Case 2														
T1	NA	19.97	0	11.33	0	0.56	NA	19.97	19.97	11.33	0.17	1.61		
T2	11.2	NA	0	11.2	0.17	0.52	11.2	NA	5.21	11.2	0	0.95		
T3	27.9	15.8	NA	27.9	0	2.22	27.9	15.8	NA	27.9	0.33	2.22		
T4	5.5	17.4	0	NA	0	0.5	5.5	17.4	17.4	NA	0	1.45		
Graph													0.95	1.56
Case 3														
T1	NA	36.3	36.3	20.6	0	2.85	NA	36.3	36.3	20.6	0.33	2.85		
T2	0	NA	5.21	11.2	0	0.47	11.2	NA	5.21	11.2	0	1.02		
T3	0	8.69	NA	15.35	0	0.51	15.35	8.69	NA	15.35	0.17	1.35		
T4	0	17.4	17.4	NA	0.33	0.58	5.5	17.4	17.4	NA	0	1.27		
Graph													1.1	1.62
Case 4														
T1	NA	36.3	36.3	20.6	0	2.85	NA	36.3	36.3	20.6	0	2.85		
T2	0	NA	2.87	6.16	0	0.25	6.16	NA	2.87	6.16	0	0.25		
T3	0	15.8	NA	27.9	0	0.6	27.9	15.8	NA	27.9	0.17	2.22		
T4	0	17.4	17.4	NA	0	0.58	5.5	17.4	17.4	NA	0	1.45		
Graph													1.07	1.69

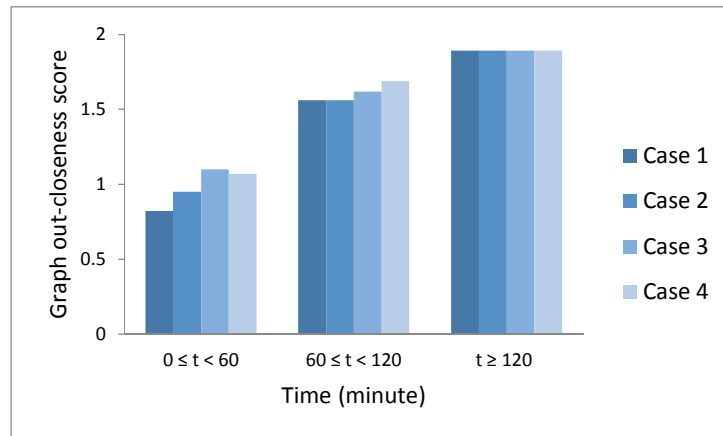


Figure 4: Comparison of graph-level out-closeness scores for Cases 1-4.

2.4. Multi-criteria decision analysis

Usually in real-life decision making problems, the criteria (objectives) influencing the decision process are in conflict; multi-criteria decision analysis (MCDA) techniques have been developed with the aim of helping decision makers deal with such decision making issues. For example, in the context of safety management of hazardous industries, an optimal allocation of safety measures to prevent/mitigate major accidents is basically dominated by a number of conflicting criteria including but not limited to the available budget, the cost of safety measures, and the effectiveness of safety measures in reducing the amount of envisaged risk. Considering a limited budget (which is almost always the case) and various types of relevant safety measures each having its own failure probability and efficiency², both the number and the configuration of MHIs to protect matter. Aside from the attributes of safety measures themselves – failure probability and efficiency – the criticality of MHIs in the initiation and propagation of major accidents (such as domino effects) and thus their contribution to the total risk (or separate on/off-site risks) play a key role in an optimal allocation of safety measures.

Due to the conflicting nature of the influential decision criteria, however, it is usually unlikely to find a decision (i.e., a set of decision variables) which satisfy the influential criteria altogether. A Pareto-optimal solution is a set of decision variables for which there is no other solution where

² Efficiency of a functioning safety measure can be defined as its capability (in percentage) of preventing/mitigating an accident as desired.

the value of a criterion can be improved without either worsening the value of other criteria or at least keeping them unchanged. A set of Pareto-optimal solutions usually contains a number of different alternatives normally prioritized based on the preferences of a decision maker. One of the basic functions of MCDA techniques is to help decision makers manifest their preferences. The method of “reference point” is one of the techniques in bi-criteria decision analysis, which intuitively represents the preferences of a decision maker based on aspiration and reservation vectors.⁽⁷⁹⁾ An aspiration vector is composed of the best values of the criteria while a reservation vector contains the worst values of the criteria. The aspiration and reservation vectors identify “Utopia” and “Nadir” points, respectively. Optionally, a decision maker can specify his preferences for criteria values between aspiration and reservation levels, based on the distances of Pareto-optimal solutions from Utopia and Nadir points. Fig. 5 displays an example of a reference point decision making, comprising Pareto-optimal solutions, i.e., points A-F, and Utopia and Nadir points. Accordingly, the solution which is the closest/farthest (e.g., using Euclidian distance) to/from the Utopia/Nadir point can be determined as the best solution:

$$\rho_{iU} = \sqrt{(x_i - x_U)^2 + (y_i - y_U)^2} \quad (5)$$

where ρ_{iU} is Euclidian distance of the i^{th} point from Utopia point; x_i and x_U are the values of the criterion X for the i^{th} point and Utopia point, respectively; y_i and y_U are the values of the criterion Y for the i^{th} point and Utopia point, respectively.

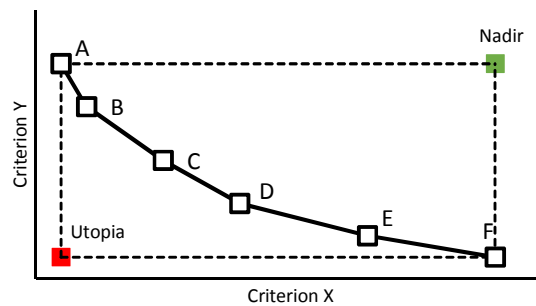


Figure 5. Bi-criteria decision analysis using the technique of reference point. The Pareto-optimal solutions, i.e., points A-F, form a Pareto front. The point with the closest distance to the Utopia

point or the point with the farthest distance to the Nadir point, based on the decision maker preferences, can be determined as the optimal solution.

3. APPLICATION OF THE METHODOLOGY

3.1 Case study

The methodology is applied to an industrial case study, in order to demonstrate the potentialities when the number of tanks is increased and possible realistic budget limitations are present, especially for the implementation of additional safety barriers. The selected case study is located in a tank farm, as represented in Fig. 6.

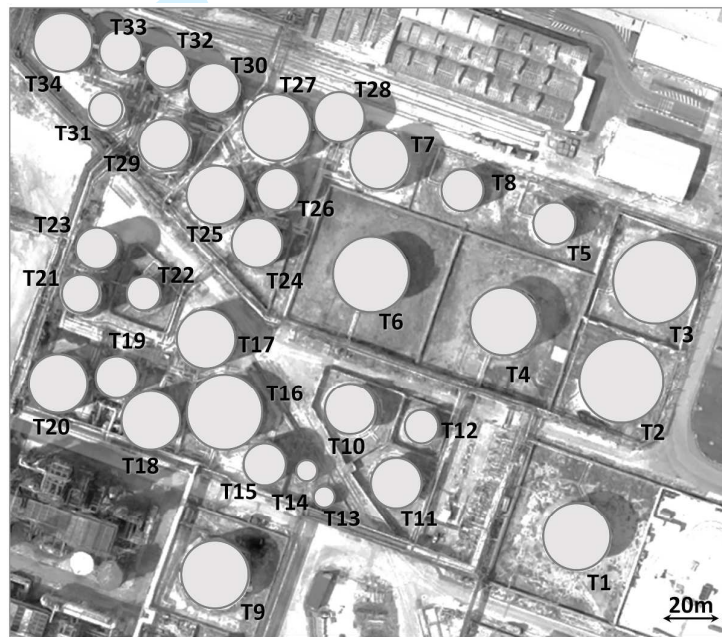


Figure 6. Layout considered for the industrial case study and identifications of tanks.

The tank farm features different types of atmospheric vertical cylindrical tanks, with nominal capacity ranging from 400 to 7600 m³ and different stored substances. Since all the contained flammables have flash points lower than 23°C, only floating roof tanks are considered.⁽⁷⁶⁾ In order to obtain a realistic evaluation, the filling level of each tank is associated with a random value in the credible operative range of 10–80%. The features of the tanks, the stored substances, and the considered inventories are summarized in Table IV. The meteorological

conditions assumed for the case study are the same as of the simplified example (e.g., $T = 15^{\circ}\text{C}$, $\text{HR} = 25\%$, and limited wind speed leading to negligible flame tilting effects).

The primary events associated with the tanks considered in the case study are pool fires following the ignition of the total inventory of the tank after a major leakage. Usually, in QRA studies it is assumed that the tank inventory will be contained in a catch basin.⁽³⁾ The layout in Fig. 6 allows to determine the size of respective catch basin areas (A_{cb} , in m^2 in Table IV) and equivalent pool diameters (D_f in Table IV). In case the tank volume exceeds the catch basin size, a maximum D_f of 70m is considered. In case multiple tanks are located in the same catch basin (e.g., see T5 and T8, or T29-T34) the primary fire is supposed to engulf the other tanks, following a conservative approach.

Table IV. Main features of the tanks considered in the case study. The costs for coating the tank with high performance passive fire protection (PFP) materials are also reported.

Tank ID	D (m)	H (m)	C (m^3)	Filling (%)	Substance	A_{cb} (m^2)	D_f (m)	A_s (m^2)	PFP cost (k€)
T1	24	12.6	5710	0.5	Crude oil	2348	55	951	390
T2	30	10.8	7630	0.7	Crude oil	1221	70	1017	417
T3	30	10.8	7630	0.7	Crude oil	1352	70	1017	417
T4	24	12.6	5710	0.49	Crude oil	2350	55	951	390
T5	15	12.6	2225	0.44	Gasoline	1757	47	593	243
T6	27	9	5182	0.26	Crude oil	2309	54	765	314
T7	21	12.6	4350	0.8	Gasoline	1041	70	830	340
T8	15	12.6	2225	0.27	Gasoline	1757	47	593	243
T9	24	12.6	5710	0.58	Gasoline	1432	70	951	390
T10	18	7.2	1843	0.39	Gasoline	665	29	408	167
T11	18	7.2	1843	0.59	Gasoline	639	29	408	167
T12	12	7.2	806	0.23	Gasoline	285	19	270	111
T13	7.5	9	397	0.76	Benzene	696	30	212	87
T14	7.5	9	397	0.14	Benzene	696	30	212	87
T15	15	12.6	2225	0.62	Toluene	2097	52	593	243
T16	27	9	5129	0.46	Methanol	2097	52	761	312
T17	21	12.6	4350	0.74	Ethanol	2097	52	830	340
T18	21	12.6	4350	0.36	Ethanol	715	70	830	340
T19	15	12.6	2225	0.32	Methanol	1098	37	593	243
T20	21	12.6	4350	0.42	Solvent	1098	37	830	340
T21	13.5	9	1282	0.28	Solvent	961	35	381	156
T22	12	7.2	806	0.44	Solvent	516	26	270	111
T23	15	18	3179	0.46	Solvent	961	35	848	348
T24	18	7.2	1843	0.72	Ethanol	3172	64	408	167

T25	21	12.6	4350	0.34	Ethanol	3172	64	830	340
T26	15	14.4	2543	0.45	Benzene	3172	64	678	278
T27	24	12.6	5710	0.77	Benzene	3172	64	951	390
T28	18	7.2	1843	0.8	Gasoline	3172	64	408	167
T29	18	7.2	1843	0.43	Toluene	3604	68	408	167
T30	18	7.2	1843	0.63	Methanol	3604	68	408	167
T31	12	7.2	806	0.23	Solvent	3604	68	270	111
T32	15	9	1590	0.42	Solvent	3604	68	424	174
T33	15	9	1590	0.54	Solvent	3604	68	424	174
T34	21	12.6	4350	0.68	Gasoline	3604	68	830	340

3.2 The applied protections and related costs

In the case study, it is assumed that all tanks are equipped with active fire protections (see Section 2.2.2), in accordance with standard industrial practices.^(76,80) Nevertheless, the update of the safety review revealed that relevant domino effect issues should be considered to improve the safety of the facility, requiring the implementation of further protective measures, in particular high performance passive fire protection (PFP) systems (see Section 2.2.1).

In order to determine the cost of PFP per unit surface of the tanks, the market analysis conducted by Paltrinieri et al.⁽⁸¹⁾ is taken as reference to identify plausible costs, considering the cost of both supply and installation of the heat resistant material. In particular, a cost range of 31-50 k€ was derived for coating a tanker for the transportation of hazardous materials, whose surface ranges typically from 120 to 170 m².^(82,83) The maximum value obtained from these figures results in a unitary cost of 410 €/m².

Based on the external surface of the tanks (A_s (m²), evaluated by assuming the entire external surface of the vertical cylindrical tank is coated), the cost to protect each tank was calculated, as reported in Table IV.

Accordingly, in order to fireproof all the tanks in the tank farm, a budget of 8.67 M€ is needed.

We may consider that only a limited budget is available, assuming about 1.3 M€ (about 15% of the total required budget), thus evaluating the cost and effectiveness of a limited number of protection combinations.

3.3 Results and discussion

3.3.1 Graph theory application

Following the procedure described in Section 2.3, and assuming that no safety barrier, either active or passive, is in place in the storage plant of Fig. 6, the credible units capable of causing domino effects and the intensities of their escalation vectors (heat radiation in this study) were identified. Accordingly, the plant was modeled as a weighted directed graph in Fig. 7. The quantities of the out-closeness and betweenness scores of the tanks are displayed in Fig. 8a and 8b, respectively. The resulted scores could have been used to assign fire protection measures to an arbitrary number of tanks with the highest out-closeness and betweenness, respectively, if the plant had to be fire protected given a sufficient budget. However, this is not the case in reality as the fire protection plans in chemical plants are largely influenced by a limited budget being available.

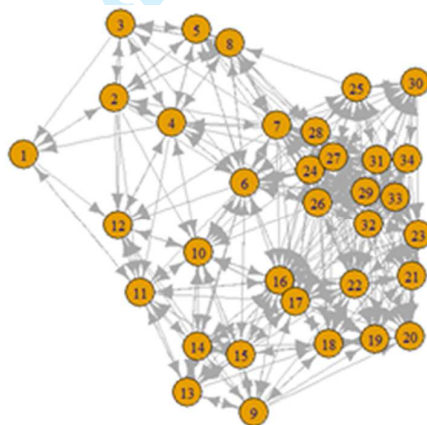
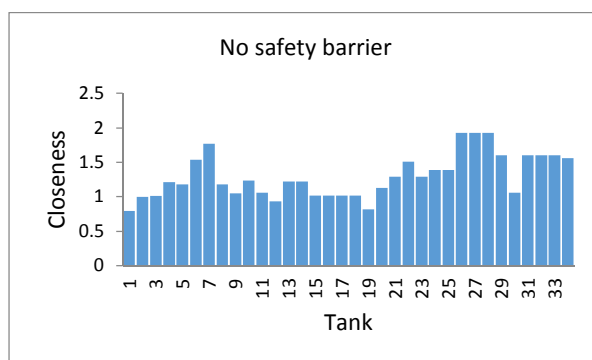
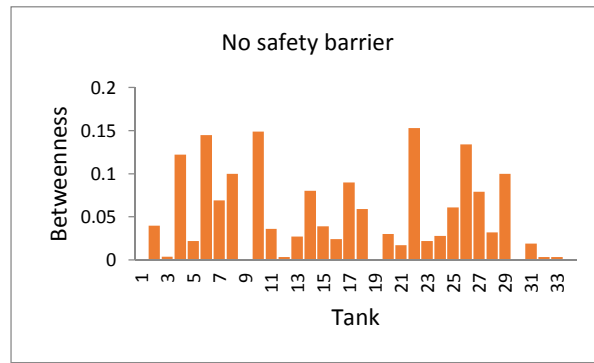


Figure 7. Storage plant of Fig. 6 as a weighted directed graph with no safety barriers in place.



(a)



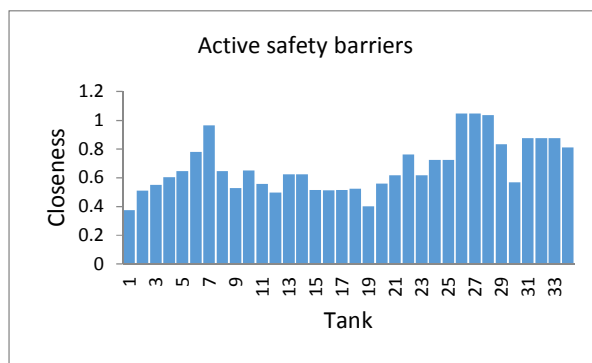
(b)

Figure 8. Graph metrics obtained for the tanks in Fig. 7 with no safety barriers in place: a) out-closeness scores b) betweenness scores.

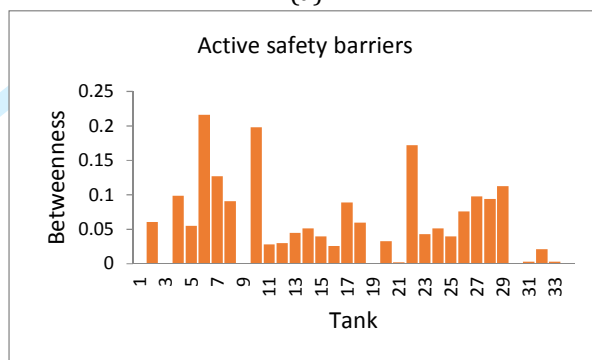
Fig. 9 illustrates the graph representation of the storage tank, knowing that all the storage tanks are already equipped with active fire safety barriers, while Fig. 10a and 10b illustrate the out-closeness and betweenness scores of the storage tanks, respectively. Through the comparison of the centrality scores in Fig. 8 with their counterparts in Fig. 10, it can be seen that the active protection of the storage tanks has not notably altered the order of the tanks regarding their out-closeness scores whereas the change in the order of the tanks based on their betweenness scores has been considerable. That is, in Fig. 8b, the first eight tanks with the highest betweenness scores are 22, 10, 6, 26, 4, 8, 29, and 17, in a descending order, whereas in Fig. 10b the sequence of the first eight tanks has changed to tanks 6, 10, 22, 7, 29, 4, 27, and 28, from the highest to the lowest.



Figure 9. Storage plant of Fig. 6 as a weighted directed graph with active safety barriers in place.



(a)



(b)

Figure 10. Graph metrics obtained for the tanks in Fig. 9 with active safety barriers in place: a) out-closeness scores b) betweenness scores.

3.3.2 Cost-effectiveness analysis of safety barriers

To further reduce the vulnerability of the storage plant to fire-induced domino effects, a number of additional passive fire safety barriers can also be allocated to the tanks with the highest betweenness scores. Under a limited budget, however, such an allocation should be carried out within a cost-effectiveness analysis to seek the most effective addition of safety barriers – in terms of both number and configuration – in compliance with the available budget.⁽⁸⁴⁾

A number of decision analysis techniques have been used for cost-effective safety management of major accidents in process/chemical industry, including analytic hierarchical process,^(85,86) limited memory influence diagram,⁽⁸⁴⁾ and linear programming.^(31,87) For the purpose of the present work, we employ the method of reference point (see Section 2.4) with the total cost of passive fire protection and the graph-level out-closeness score as the two criteria in the decision analysis. To this end, eight decision alternatives (plans) are defined, namely Plan 1 to Plan 8. Each plan corresponds to the fireproofing of the cumulative number of the first eight tanks with

the highest betweenness scores in Fig. 10b. Hence, Plan 1 refers to the fireproofing of Tank 6; Plan 2 refers to the fireproofing of both Tanks 6 and 10; Plan 3 refers to the fireproofing of Tanks 6, 10, and 22; and so on.

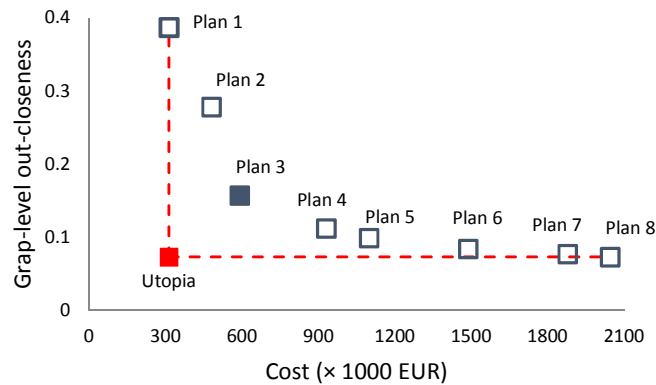


Figure 11. Cost-effectiveness analysis to determine an optimal fireproofing plan.

Having the cost of fireproofing of each tank in Table IV, the total cost of each plan can be calculated. Further, employing the methodology described in Section 2.3.3, the out-closeness scores of graphs resulted from the implementation of each fireproofing plan can be calculated. Fig. 11 depicts the values of the decision criteria, i.e., the cost and the graph-level out-closeness score, for each fireproofing plan. As can be seen from Fig. 11, the more tanks to fireproof, the higher the cost of fireproofing and thus the lower the graph-level out-closeness score, which in turn implies the less vulnerability of the plant to fire-induced domino effects. Using the Utopia point as the reference point, as evident from Fig. 11, Plan 3 is the closest point to Utopia and thus can be identified as the optimal decision alternative.

3.3.3 Discussion

In previous sections, the efficacy of the graph metrics – out-closeness and betweenness – was demonstrated in supporting a detailed vulnerability analysis of chemical plants with regard to fire-induced domino effects. The results obtained can be considered from two perspectives.

From one hand, the developed methodology can be employed as a practical tool for a preliminary screening of MHIs in a chemical plant in terms of their contribution to the plant

vulnerability during domino effects. As a result, the plant major criticalities as well as installation vulnerabilities and potential “weak points” can be determined in a quick fashion. From the other hand, the vulnerability of the installations and thus that of the plant can be reduced via effective allocation of active and passive fire safety measures, the former to installations with the highest out-closeness scores while the latter to ones with the highest betweenness scores.

It should be noted that due to the deterministic nature of the present study, neither the failure probability nor the efficiency of fire protection measures was considered in the calculation of graph centrality scores. This shortcoming, however, does not seem to influence the order of critical installations as long as the same types of safety measures, whether active or passive, are used for the installations of interest. Nonetheless, one may take into account the failure probability of safety measures, for example, by replacing the weight of the respective edge with an “expected” weight in the graph. For the sake of clarity, consider tanks T1 and T2 in Fig. 12a in which the intensity of heat radiation from T1 to T2 is 20 kW/m^2 . In case of active fire protection of T1, the intensity of heat radiation received by T2 will reduce to $20 \times 0.55 = 11 \text{ kW/m}^2$ (Fig. 12b). Assuming a failure probability of 0.1, for illustrative purposes, for the active fire protection, the expected value of heat radiation received by T2 can be calculated as $20 \times 0.1 + 11 \times 0.9 = 11.9 \text{ kW/m}^2$. Accordingly, the weight of the corresponding edge from T1 to T2 will change from $10/11 = 0.91$ to $10/11.9 = 0.84$.

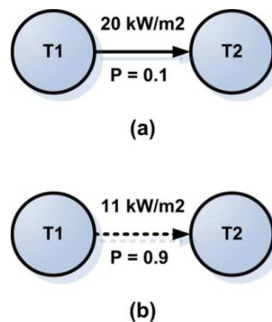


Figure 12: Heat radiation intensity without (a) and with (b) the operation of active fire protection.

1
2
3 In the present study, we took advantage of safety measures such as rim seal water sprinkler
4 (active protection) and fireproof coating (passive protection). However, the developed
5 methodology can readily be extended to account for a variety of active and passive fire
6 protection measures including emergency response actions by manipulating the weight of
7 relevant arcs. Although being inspired by a work of Khakzad and Reniers,⁽⁴⁹⁾ the present study
8 outdoes previous work as its dynamic approach facilitates not only the modeling of the
9 temporal degradation of fire protection measures but also the incorporation of the flammable
10 contents of involved MHIs. The latter can make a notable difference in the cost-effective
11 allocation of safety measures since the MHIs with lower flammable inventories are likely to be
12 excluded from the graph within initial time intervals (see Fig. 3) due to the burn-out of their
13 contents, thus no longer contributing to domino effects. This modeling feature, however, did not
14 manifest in the current study since even the burn-out time of the storage tanks with the lowest
15 flammable inventories, e.g., tanks 12 (572 min) and 13 (1234 min) in Table IV, are far beyond
16 the degradation times (60 min for passive and 120 min for active fire protections) used in the
17 dynamic graph theory approach.
18
19
20
21
22
23
24
25
26
27
28
29
30
31
32
33
34
35

36 5. CONCLUSIONS

37
38 In the present study we demonstrated an application of graph theory and multi-criteria decision
39 analysis to cost-effective fire protection of chemical plants, especially with regard to fire-
40 induced domino effects. Representing the major hazardous installations of a chemical plant (e.g.,
41 storage tanks) and the escalation vectors (e.g., heat radiation) as vertices and edges of a
42 weighted directed graph, respectively, the vertex-level out-closeness and betweenness scores
43 can be used to identify the most critical installations in the context of domino effects. Likewise,
44 the graph-level out-closeness score can be used to measure the vulnerability of the entire
45 chemical plant to domino effects. The installations with the highest out-closeness and
46 betweenness scores contribute the most to the initiation and the propagation, respectively, of
47 domino effects. As a result, the control/suppression of the former by means of active fire
48
49
50
51
52
53
54
55
56
57
58
59
60

1
2
3 protection (rim seal water sprinklers in this study) and the insulation of the latter by means of
4
5 passive fire protection (fireproof coating in this study) prove to be the most effective fire
6
7 protection strategy within chemical plants. We also illustrated that the results of the graph
8
9 analysis can further be prioritized in a multi-criteria decision analysis to determine the most
10
11 cost-effective fire protection strategies under a limited budget. The application of the
12
13 methodology was exemplified via a large real-life storage plant, showing the practicality and
14
15 efficacy of the methodology in cost-effective fire protection of complex chemical plants.
16
17
18
19
20
21
22
23
24
25
26
27
28
29
30
31
32
33
34
35
36
37
38
39
40
41
42
43
44
45
46
47
48
49
50
51
52
53
54
55
56
57
58
59
60

For Peer Review

REFERENCES

1. Delvosalle C. A methodology for the identification and evaluation of domino effects. Brussels, Belgium: Belgian Ministry of Employment and Labour; 1998.
2. Gledhill J, Lines I. Development of methods to assess the significance of domino effects from major hazard sites. London, UK: Health and Safety Executive, HM Stationery Office; 1998.
3. Lees FP. Loss prevention in the process industries. 2nd ed. Oxford: Butterworth - Heinemann; 1996.
4. Khan FI, Abbasi SA. Models for domino effect analysis in chemical process industries. *Process Saf Prog* 1998;17:107–23.
5. Hemmatian B, Abdolhamidzadeh B, Darbra RM, Casal J. The significance of domino effect in chemical accidents. *J Loss Prev Process Ind* 2014;29:30–8.
6. Darbra RM, Palacios A, Casal J. Domino effect in chemical accidents: Main features and accident sequences. *J Hazard Mater* 2010;183:565–73.
7. Bagster DF, Pitblado RM. Estimation of domino incident frequencies - an approach. *Process Saf Environ Prot Trans Inst Chem Eng Part B* 1991;69:195–9.
8. Khan FI, Abbasi SA. The world's worst industrial accident of the 1990s: What happened and what might have been - A quantitative study. *Process Saf Prog* 1999;18:135–45.
9. Casal J, Darbra R-M. Analysis of Past Accidents and Relevant Case-Histories. *Domino Eff. Process Ind. Model. Prev. Manag.*, 2013, p. 12–29.
10. Reniers G, Cozzani V. Features of Escalation Scenarios. *Domino Eff. Process Ind. Model. Prev. Manag.*, Amsterdam, The Netherlands: Elsevier B.V.; 2013, p. 30–42.
11. Necci A, Cozzani V, Spadoni G, Khan F. Assessment of domino effect: State of the art and research Needs. *Reliab Eng Syst Saf* 2015;143:3–18.
12. European Commission. European Parliament and Council Directive 2012/18/EU of 4 July 2012 on control of major-accident hazards involving dangerous substances, amending and subsequently repealing council directive 96/82/EC. 2012.
13. Contini, S., Boy, S., Atkinson, M., Labath, N., Banca, M., Nordvik JP. Domino effect evaluation of major industrial installations: a computer aided methodological approach. *Proc. Eur. Semin. Domino Eff.*, Leuven, B: 1996.
14. Egidi, D., Foraboschi, F.P., Spadoni, G., Amendola A. The ARIPAR project: analysis of the major accident risks connected with industrial and transportation activities in the Ravenna area. *Reliab Eng Syst Saf* 1995;49:75–89.
15. Latha P, Gautam G, Raghavan K V. Strategies for the quantification of thermally initiated cascade effects. *J Loss Prev Process Ind* 1992;5:18–27..
16. RP Authority. COVO Risk Analysis of Six Potentially Hazardous Industrial Objects in the Rijnmond Area, A Pilot Study. A Report to the Rijnmond Public Authority. Schiedam, NL: Central Environmental Control Agency; 1982.
17. Cozzani V, Salzano E. The quantitative assessment of domino effects caused by overpressure: Part I. Probit models. *J Hazard Mater* 2004;107:67–80.
18. Tugnoli A, Gubinelli G, Landucci G, Cozzani V. Assessment of fragment projection hazard: Probability distributions for the initial direction of fragments. *J Hazard Mater* 2014;279C:418–27.
19. Tugnoli A, Milazzo MF, Landucci G, Cozzani V, Maschio G. Assessment of the hazard due to fragment projection: A case study. *J Loss Prev Process Ind* 2014;28:36–46.
20. Landucci G, Gubinelli G, Antonioni G, Cozzani V. The assessment of the damage probability of storage tanks in domino events triggered by fire. *Accid Anal Prev* 2009;41:1206–15.
21. Nguyen QB, Mebarki A, Saada RA, Mercier F, Reimeringer M. Integrated probabilistic framework for domino effect and risk analysis. *Adv Eng Softw* 2009;40:892–901.
22. Mebarki A, Jerez S, Matasic I, Prodhomme G, Reimeringer M. Explosions and structural fragments as industrial hazard: Domino effect and risks. *Procedia Eng.*, vol. 45, 2012, p. 159–66.
23. Ramírez-Camacho J, Pastor E, Casal J, Amaya-Gómez R, Muñoz-Giraldo F. Analysis of domino

- effect in pipelines. *J Hazard Mater* 2015;298:210–20.
24. Cozzani V, Gubinelli G, Antonioni G, Spadoni G, Zanelli S. The assessment of risk caused by domino effect in quantitative area risk analysis. *J Hazard Mater* 2005;127:14–30.
25. Antonioni G, Spadoni G, Cozzani V. Application of domino effect quantitative risk assessment to an extended industrial area. *J Loss Prev Process Ind* 2009;22:614–24.
26. Cozzani V, Antonioni G, Landucci G, Tugnoli A, Bonvicini S, Spadoni G. Quantitative assessment of domino and NaTech scenarios in complex industrial areas. *J Loss Prev Process Ind* 2014;28:10–22.
27. Abdolhamidzadeh B, Abbasi T, Rashtchian D, Abbasi SA. A new method for assessing domino effect in chemical process industry. *J Hazard Mater* 2010;182:416–26.
28. Khakzad N, Khan F, Amyotte P, Cozzani V. Domino effect analysis using Bayesian networks. *Risk Anal* 2013;33:292–306.
29. Khakzad N, Khan F, Amyotte P, Cozzani V. Risk management of domino effects considering dynamic consequence analysis. *Risk Anal* 2014;34(6): 1128–1138.
30. Khakzad N. Application of dynamic Bayesian network to risk analysis of domino effects in chemical infrastructures. *Reliab Eng Syst Saf* 2015;138:263–72.
31. Janssens J, Talarico L, Reniers G, Sorensen K. A decision model to allocate protective safety barriers and mitigate domino effects. *Reliab Eng Syst Saf* 2015;143:44–52.
32. Tugnoli A, Khan F, Amyotte P, Cozzani V. Safety assessment in plant layout design using indexing approach: Implementing inherent safety perspective. Part 2-Domino Hazard Index and case study. *J Hazard Mater* 2008;160:110–21.
33. Tugnoli A, Khan F, Amyotte P, Cozzani V. Safety assessment in plant layout design using indexing approach: Implementing inherent safety perspective. Part 1 - Guideword applicability and method description. *J Hazard Mater* 2008;160:100–9.
34. Cozzani V, Tugnoli A, Salzano E. The development of an inherent safety approach to the prevention of domino accidents. *Accid Anal Prev* 2009;41:1216–27.
35. Reniers GLL, Audenaert A. Preparing for major terrorist attacks against chemical clusters: Intelligently planning protection measures w.r.t. domino effects. *Process Saf Environ Prot* 2013.
36. Tugnoli A, Cozzani V, Landucci G. A consequence based approach to the quantitative assessment of inherent safety. *AIChE J* 2007;53:3171–82.
37. Tugnoli A, Landucci G, Salzano E, Cozzani V. Supporting the selection of process and plant design options by Inherent Safety KPIs. *J Loss Prev Process Ind* 2012;25:830–42.
38. Kletz TA. What You Don't Have, Can't Leak. *Chem Ind* 1978;1:287–92.
39. CCPS - Center of Chemical Process Safety. Inherently Safer Chemical Processes- A Life Cycle Approach. New York, NY: American Institute of Chemical Engineers - Center of Chemical Process Safety; 1996.
40. Di Padova A, Tugnoli A, Cozzani V, Barbaresi T, Tallone F. Identification of fireproofing zones in Oil&Gas facilities by a risk-based procedure. *J Hazard Mater* 2011;191:83–93.
41. Tugnoli A, Cozzani V, Di Padova A, Barbaresi T, Tallone F. Mitigation of fire damage and escalation by fireproofing: A risk-based strategy. *Reliab Eng Syst Saf* 2012;105:25–35.
42. Pavlova Y, Reniers G. A sequential-move game for enhancing safety and security cooperation within chemical clusters. *J Hazard Mater* 2011;186:401–6.
43. Reniers GLL, Dullaert W. Knock-on accident prevention in a chemical cluster. *Expert Syst Appl* 2008;34:42–9.
44. Reniers G, Dullaert W, Karel S. Domino effects within a chemical cluster: A game-theoretical modeling approach by using Nash-equilibrium. *J Hazard Mater* 2009; 167: 289–93.
45. Landucci G, Argenti F, Tugnoli A, Cozzani V. Quantitative assessment of safety barrier performance in the prevention of domino scenarios triggered by fire. *Reliab Eng Syst Saf* 2015;143:30–43.
46. Landucci G, Argenti F, Spadoni G, Cozzani V. Domino effect frequency assessment: the role of safety barriers. *J Loss Prev Process Ind* 2016.
47. CCPS - Center of Chemical Process Safety. Layer of protection analysis: simplified process risk assessment. New York, NY: American Institute of Chemical Engineers - Center of

- 1
2
3 Chemical Process Safety; 2001.
- 4 48. De Dianous V, Fiévez C. ARAMIS project: A more explicit demonstration of risk control
5 through the use of bow-tie diagrams and the evaluation of safety barrier performance. *J*
6 *Hazard Mater* 2006;130:220–33.
- 7 49. Khakzad N, Reniers G. Using graph theory to analyze the vulnerability of process plants in
8 the context of cascading effects. *Reliab Eng Syst Saf* 2015;143:63–73.
- 9 50. Yazdani A, Otoo RA, Jeffrey P. Resilience enhancing expansion strategies for water
10 distribution systems: A network theory approach. *Environ Model Softw* 2011; 26:1574–
11 82.
- 12 51. Johansson J, Hassel H, Zio E. Reliability and vulnerability analyses of critical infrastructures:
13 Comparing two approaches in the context of power systems. *Reliab Eng Syst Saf*
14 2013;120:27–38.
- 15 52. Khakzad N, Reniers G, Abbassi R, Khan F. Vulnerability analysis of process plants subject to
16 domino effects. *Reliab Eng Syst Saf* n.d.
- 17 53. Landucci G, Cozzani V, Birk M. Heat Radiation Effects. *Domino Eff. Process Ind. Model. Prev.*
18 *Manag.*, Amsterdam, The Netherlands: Elsevier; 2013, p. 70–115.
- 19 54. Freeman L. Centrality in social networks I: Conceptual clarification. *Soc Networks* 1979;
20 1:215–39.
- 21 55. Kim JW, Jung W. A taxonomy of performance influencing factors for human reliability
22 analysis of emergency tasks. *J Loss Prev Process Ind* 2003;16:479–95.
- 23 56. Musharraf M, Khan F, Veitch B, Mackinnon S, Imtiaz S. Human factor risk assessment during
24 emergency condition in harsh environment. *Proc. ASME 2013 32nd Int. Conf. Ocean.*
25 *Offshore Arct. Eng. (OMAE 2013)*, June 9-14, 2013, Nantes, Fr., New York, NY: American
26 Society of Mechanical Engineers; 2013, p. 1–9.
- 27 57. Brown DF, Dunn WE. Application of a quantitative risk assessment method to emergency
28 response planning. *Comput Oper Res* 2007;34:1243–65.
- 29 58. CCPS - Center of Chemical Process Safety. Guidelines for engineering design for process
30 safety. New York, NY: American Institute of Chemical Engineers - Center of Chemical
31 Process Safety; 2001.
- 32 59. Gomez-Mares M, Tugnoli A, Landucci G, Cozzani V. Performance Assessment of Passive Fire
33 Protection Materials. *Ind Eng Chem Res* 2012;51:7679–89.
- 34 60. Gomez-Mares M, Tugnoli A, Landucci G, Barontini F, Cozzani V. Behavior of intumescent
35 epoxy resins in fireproofing applications. *J Anal Appl Pyrolysis* 2012;97:99–108.
- 36 61. Birk AM, Poirier D, Davison C. On the thermal rupture of 1.9 m³ propane pressure vessels
37 with defects in their thermal protection system. *J Loss Prev Process Ind* 2006;19:582–97.
- 38 62. Birk A. Scale effects with fire exposure of pressure-liquified gas tanks. *Loss Prev Process Ind*
39 1995;8:275–90.
- 40 63. Gómez-Mares M, Tugnoli A, Larchera S, Landucci G, Barontini F, Cozzani V. Enhanced
41 modelling of exposed PFP coatings based on bench-scale fire-tests. *Chem Eng Trans*
42 2012;26:321–6.
- 43 64. Argenti F, Landucci G. Experimental and numerical methodology for the analysis of
44 fireproofing materials. *J Loss Prev Process Ind* 2014; 28: 60–71.
- 45 65. Tugnoli A, Landucci G, Villa V, Argenti F, Cozzani V. The performance of inorganic passive
46 fire protections: An experimental and modelling study. *Chem Eng Trans* 2013;32:427–32.
- 47 66. Roberts A, Medonos S, Shirvill LC. Review of the Response of Pressurised Process Vessels
48 and Equipment to Fire Attack OFFSHORE TECHNOLOGY REPORT - OTO 2000 051.
49 Buxton UK: Health and Safety Laboratory, Fire and Explosion Group; 2000.
- 50 67. NORSOK-standards. Standard S-001 - Technical Safety. 4th ed. Lysaker, NO: NORSOK; 2008.
- 51 68. Nolan DP. Handbook of fire and explosion protection engineering principles for oil, gas,
52 chemical and related facilities. Oxford (UK): Elsevier; 1996.
- 53 69. NFPA-National Fire Protection Association. NFPA 15 - standard for water spray fixed
54 systems for fire protection. Quincy (MA): NFPA; 2009.
- 55 70. Necci A, Antonioni G, Krausmann E, Argenti F, Landucci G, Cozzani V. Accident scenarios
56 caused by lightning impact on atmospheric storage tanks. *Chem Eng Trans* 2013;32:139–
57
58
59
60

- 1
2
3 44.
4 71. Roberts TA. Effectiveness of an enhanced deluge system to protect LPG tanks and sensitivity
5 to blocked nozzles and delayed deluge initiation. *J Loss Prev Process Ind* 2004;17:151–8.
6 72. Roberts TA. Directed deluge system designs and determination of the effectiveness of the
7 currently recommended minimum deluge rate for the protection of LPG tanks. *J Loss*
8 *Prev Process Ind* 2004;17:103–9.
9 73. SCI-Steel Construction Institute. Availability and properties of passive and active fire
10 protection systems, OTI92607. London, UK: Health and Safety Executive, HM Stationery
11 Office, London, UK; 1992.
12 74. Liu Z, Kim A. A review of water mist fire suppression systems - fundamental studies. *J Fire*
13 *Prot Eng* 2000;10:32–50.
14 75. Mawhinney JR, Dlugogorski BZ, Kim A. A closer look at the fire extinguishing properties of
15 water mist. *Fire Saf. Sci. - Proc. 4th Int. Symp.*, London, UK: International Association for
16 Fire Safety Science; 1994, p. 47–60.
17 76. Oil Industry Safety Directorate. OISD STD 116 - Fire protection facilities for petroleum
18 refineries and oil/gas processing plants. New Delhi: OISD; 1999.
19 77. Csardi G, Nepusz T. The igraph software package for complex network research. *Int J*
20 *Complex Syst* 2006:1695.
21 78. R Development Core Team. R: a language and environment for statistical computing, R
22 Foundation for Statistical Computing. Vienna, Austria: R Foundation for Statistical
23 Computing; 2009.
24 79. Deb K. Multi-Objective optimization using evolutionary algorithms. New York, NY: John
25 Wiley & Sons; 2001.
26 80. Necci A, Argenti F, Landucci G, Cozzani V. Accident scenarios triggered by lightning strike on
27 atmospheric storage tanks. *Reliab Eng Syst Saf* 2014;127:30–46.
28 81. Paltrinieri N, Bonvicini S, Spadoni G, Cozzani V. Cost-benefit analysis of passive fire
29 protections in road LPG transportation. *Risk Anal* 2012;32:200–19.
30 82. Paltrinieri N, Landucci G, Molag M, Bonvicini S, Spadoni G, Cozzani V. Risk reduction in road
31 and rail LPG transportation by passive fire protection. *J Hazard Mater* 2009;167:332–44.
32 83. Landucci G, Molag M, Cozzani V. Modeling the performance of coated LPG tanks engulfed in
33 fires. *J Hazard Mater* 2009;172:447–56.
34 84. Khakzad N, Reniers G. Cost-effective allocation of safety measures in chemical plants w.r.t.
35 land-use planning. *Saf Sci* 2015. doi:http://dx.doi.org/10.1016/j.ssci.2015.10.010.
36 85. Khakzad N, Reniers G. Application of Bayesian network and multi-criteria decision analysis
37 to risk-based design of chemical plants. *Chem Eng Trans* 2016;48.
38 86. Khakzad N, Reniers G. Risk-based design of process plants with regard to domino effects and
39 land use planning. *J Hazard Mater* 2015;299:289–97.
40 87. Zhu Y, Khakzad N, Khan F, Amyotte P. Risk-based optimal safety measure allocation for dust
41 explosions. *Saf Sci* 2015;74:79–92.
42
43
44
45
46
47
48
49
50
51
52
53
54
55
56
57
58
59
60